Mechanics of Advanced Composite Structures

Semnan University

journal homepage: http://MACS.journals.semnan.ac.ir

High-order Analysis of Linear Vibrations of Moderately Thick Sandwich Panel with an Electro-rheological Core

M. Keshavarzian [a], M.M. Najafizadeh [b], K. Khorshidi [c, *], P. Yousefi [d], M. Alavi [e]

[a,b,d] *Department of Mechanical Engineering, Arak Branch, Islamic Azad University, Arak, Iran*
[c] *Department of Mechanical Engineering, Faculty of Engineering, Arak University, Arak, Iran*
[e] *Department of Mathematics, Arak Branch, Islamic Azad University, Arak, Iran*

KEYWORDS

Free vibration
Sandwich panel
Electro-rheological

ABSTRACT

In this study, the frequency response of rectangular sandwich plates with multi-layer face sheets and electrorheological (ER) fluid cores is investigated. The assumed electro-rheological fluid as a core is capable of changing the stiffness and damping of structures. In modelling the sandwich panel implemented for the first time, first-order shear deformation theory and the second Frostig's model are applied for the face sheets and thick cores, respectively. The sandwich panel under study is supposed to simply support boundary in all edges, and the Galerkin approach is implemented for discretizing the problem. In the result section, impacts of various parameters such as electric field, aspect ratio, the thickness of the ER layer, and thickness ratio on vibrational characteristics of the structure are discussed in detail. The obtained results highlight the notable effects of the electric field on natural frequencies, which can make the structure flexible within the desired range. It is also pointed out that the dynamic behavior and stability of the system can be controlled by changing the magnitude of the ER fluid layer.

1. Introduction

A sandwich structure, whether beam or sheet, consists of two thin surface sheets of a rigid structure that bonded to a soft, flexible, and relatively thick core. Surfaces are usually made of thin solid metal sheets or composite laminate sheets. The cores are also often made of light polymers, foams, or honeycomb structures.

The higher order sandwich panel theory was developed by Frostig et al. [1], who considered two types of computational models to describe governing equations of the core layer. The second model assumed a polynomial description of the displacement fields in the core, which was based on the displacement fields of the first model. The improved higher-order sandwich plate theory (IHSAPT), applying the first-order shear deformation theory for the face sheets, was introduced by Malekzadeh et al. [2]. The first-order shear deformation theory [3, 4] incorporates the shear deformation effects, but it considers a constant transverse shear deformation along the thickness of the plate. Thus, it violates stress-free conditions at the bottom and top of the plate and needs a shear correction factor. To get accurate results and to avoid using shear correction factor, the higher-order shear deformation theory (HSDT) was developed. Reddy [5] employed a parabolic shear stress distribution along the thickness of the plate. His model didn't need a shear correction factor because of satisfying free stress conditions at the bottom and top of the plate. The mechanical behavior of sheets is often studied and analyzed using plate theories. Most plate and shell theories are based on a kinematic assumption of displacement or the deformation of the object in three dimensions [6]. Sayyad and Ghugal [7, 8] used exponential and trigonometric shear deformation theories for bending and free vibration analysis of thick plates. Ghasemi and Mohandes [9] studied the free vibration analysis of fiber-metal laminate thin circular cylindrical shells with simply supported boundary conditions based on Love's first approximation shell theory. The result demonstrated that with an increase in the axial and circumferential wavenumber, the gap between forward and backward frequencies increased. In addition, with an increase in the axial-wavenumber, the natural frequency decreased and then increased. Nonlinear free vibration of an Euler-Bernoulli composite

* Corresponding author. Tel.: +98-86-32625720; Fax: +98-86-34173450
E-mail address: k-khorshidi@araku.ac.ir

DOI: 10.22075/MACS.2020.20131.1247
Received 2020-04-03; Received in revised form 2020-06-27; Accepted 2020-07-13

beam undergoing finite strain subjected to different boundary conditions was studied by Ghasemi et al. [10]. Free Vibration of Sandwich Panels with Smart Magneto-Rheological Layers and Flexible Cores has been studied by Payganeh et al. [11]. They used the exponential shear deformation theory in their analysis. Mozaffari et al. [12] examined the memory alloys on the free vibration behavior of flexible-core sandwich-composite panels. Qajar et al. [13] also analyzed the dynamic response of double curved composite shells under low- velocity impact. Khorshidi et al. [14] investigated the electro-mechanical free vibrations of composite rectangular piezoelectric nanoplate using modified shear deformation theories. One of the most important damages of sandwich structures is the separation in the middle layer between the core and the shell. The reason for this separation is the difference in Young's modulus ratio between the core and the face sheet. The use of a material with high shear stress tolerance in the core weakens the adhesion of the middle layer. The core use of FGM or ER smart fluids eliminates all of these problems. Under the influence of electric fields, intelligent fluids exhibit rapid changes in hardness and damping properties. These fluids are also very suitable for vibration control over very large ranges. The concept of material-based ER adaptive structures was first put forward by Carlson et al. [15] in a patent filed with the US Patent Center. Most of the work published in the last few years has focused mainly on the experimental and theoretical aspects of ER adaptive structures [16-17]. However, research on adaptive MR sandwich structures is in its infancy. Some research has investigated the vibrational and damping properties of ER and MR materials with adaptive structures [18-19]. Yeh et al. [20] examined the vibrational properties and modal damping coefficient of circular sandwich sheets with orthotropic face sheets and ER core. Ramkumar and Gensan [21] used ER fluids as the core of a sandwich hollow column wall and compared the performance of ER fluid application with viscoelastic materials in changing the vibrational properties of the column. The most recent work on MR fluids is a study by-Rajamohan et al. [22]. They modeled a sandwich beam with an MR core, considering the shear effects of the MR binding layer on the core and applying the equivalent shear modulus. They applied the finite element method to solve the problem and investigated the effects of magnetic field intensity on vibrational properties for different boundary conditions and forced loading. Free vibration analysis of porous laminated rotating circular cylindrical shells has been done by Ghasemi and Meskini [23]. Also, for the first time, Rajamohan et al. [24] investigated the vibrational properties of a partially filled MR sandwich beam both experimentally and via the finite element method. Rajamohan et al. [25] were the first who explored the model presented in [24] to find the optimal location of partial MR layers for maximizing the modal damping coefficient of sandwich beams. They tested the optimal location of the partial MR layers to maximize the first five modal damping coefficients of the beam separately and simultaneously.

In this study, based on the displacement field of each layer, the kinetic energy and strain energy are separately obtained for each layer. Using total kinetic energy and total strain energy, in the Hamiltonian principle, the structural motion equation is obtained. Primary attention is focused on the effects of electric field magnitude, geometric aspect ratio, and ER core layer thickness on dynamic characteristics of the sandwich plate. Natural frequencies and loss factor for the electric fields, as well as the ratio of different thicknesses are calculated by Galerkin analytical method. As the applied electric field increases, the natural frequency of the sandwich plate increases, and the modal loss factor decreases. With increasing the thickness of the ER layer, the natural frequencies of the sandwich plate are decreased.

2. Obtaining the equations that govern the problem

The assumptions for modeling the problem are as follows:

- Face sheets are elastic and can be an isotropic, orthotropic, or composite material.
- It is assumed that there is no slipping between the elastic layers of the ER layer.
- Transverse displacement is assumed to be identical for all points on a hypothetical cross-sectional area.
- It is assumed that there is no normal stress in the ER layer.
- The ER is modeled as a linear viscoelastic material in pre-submission conditions.
- The ER used in the Core completely covers the core with the displacements considered linear and small, and the face sheet is assumed to be thin.

The improved high-order theory of sandwich plates has been used to derive the governing equations. According to this theory, for composite sheets, the first-order shear deformation theory is used while the displacement sentence term, which is based on Frostig's second-order displacements, is used for the core. In this case, the unknowns are fixed polynomial coefficients. Further, in this study, the displacements of the face sheets for the core and the surfaces are assumed to be very dynamic. Figure 1 shows a flat sandwich sheet with two laminated composite sheets on its faces.

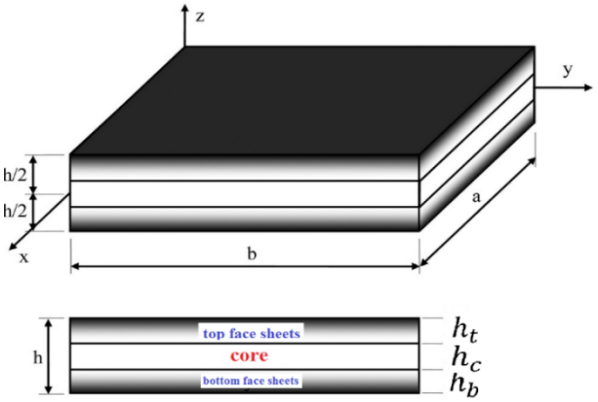

Fig. 1. Sandwich plate with laminated composite sheets on the surfaces

The thickness of the top sheet, the bottom sheet, and the core are as follows: h_t, h_b, h_c. The sandwich panel is supposed to have length a, width b, and total thickness h. The orthogonal co-ordinates $(x_i, y_i, z_i \;\; i = t, b, c)$ are also shown in Fig. 1. In this study, the t index corresponds to the upper sheet, the b index to the lower sheet, and the c index to the core.

2.1. Displacement fields and strain relations - Displacement for face sheets and core

According to the first-order shear deformation theory, the displacements u, v, and w face sheets in the x, y, and z directions assume small linear displacements as Eq. (1):

$$\begin{aligned} u_i(x,z,y,t) &= u_0^i(x,y,t) + z_i\phi_x^i(x,y,t) \\ v_i(x,z,y,t) &= v_0^i(x,y,t) + z_i\phi_y^i(x,y,t) \\ w_i(x,z,y,t) &= w_0^i(x,y,t)\,;(i=t,b) \end{aligned} \tag{1}$$

where z_i is the vertical coordinate of each face sheet (i = t, b), measured upward from the mid-plane of each face sheet. Kinematic equations of the face sheets are as follows:

$$\begin{aligned} &\varepsilon_{xx}^i = \varepsilon_{0xx}^i + z_i k_{xx}^i \\ &\varepsilon_{yy}^i = \varepsilon_{0yy}^i + z_i k_{yy}^i, \quad \varepsilon_{zz}^i = 0 \\ &\gamma_{xy}^i = 2\varepsilon_{xy}^i = \varepsilon_{0xy}^i + z_i K_{xy}^i\,, \qquad i = t,b \\ &\gamma_{xz}^i = 2\varepsilon_{xz}^i = \varepsilon_{0xz}^i\,, \\ &\gamma_{yz}^i = 2\varepsilon_{yz}^i = \varepsilon_{0yz}^i\,, \\ &\varepsilon_{0xx}^i = \frac{\partial u_0^i}{\partial x}, \varepsilon_{0yy}^i = \frac{\partial v_0^i}{\partial y} \\ &\varepsilon_{0xy}^i = \frac{\partial v_0^i}{\partial x} + \frac{\partial u_0^i}{\partial y}, \varepsilon_{0xz}^i = \frac{\partial w_0^i}{\partial x} + \phi_x^i \\ &\varepsilon_{0yz}^i = \frac{\partial w_0^i}{\partial y} + \phi_y^i\,,\; K_{xy}^i = \frac{\partial w_x^i}{\partial x} \\ &K_{yy}^i = \frac{\partial w_y^i}{\partial y}, K_{xy}^i = \frac{\partial w_y^i}{\partial x} + \frac{\partial w_x^i}{\partial y} \end{aligned} \tag{2, 3}$$

As can be seen, ε_{zz} for the face sheets are equal to zero. This means that the face sheets are assumed to be rigid in the Z direction. Displacement relations are based on Frostig's second model for the thick core in the form of Eqs. (4) [26]:

$$\begin{aligned} u_c(x,y,z,t) &= u_0^c(x,y,t) \\ &\quad + z_c u_1^c(x,y,t) \\ &\quad + z_c^2 u_2^c(x,y,t) \\ &\quad + z_c^3 u_3^c(x,y,t) \\ v_c(x,y,z,t) &= v_0^c(x,y,t) \\ &\quad + z_c v_1^c(x,y,t) \\ &\quad + z_c^2 v_2^c(x,y,t) \\ &\quad + z_c^3 v_3^c(x,y,t) \\ w_c(x,y,z,t) &= w_0^c(x,y,t) \\ &\quad + z_c w_1^c(x,y,t) \\ &\quad + z_c^2 w_2^c(x,y,t) \end{aligned} \tag{4}$$

The kinematic relationships of the core in a sandwich panel are based on the relation of small deformations:

$$\begin{aligned} &\varepsilon_{xx}^c = \left(\frac{\partial u_c}{\partial x}\right) \\ &\varepsilon_{yy}^c = \left(\frac{\partial v_c}{\partial y}\right)\,, \varepsilon_{zz}^c = w_1^c + 2z w_2^c, \\ &\gamma_{xy}^c = 2\varepsilon_{xy}^c = \frac{\partial v_c}{\partial x} + \frac{\partial u_c}{\partial y} \\ &\gamma_{xz}^c = 2\varepsilon_{xz}^c = \left(\frac{\partial w_c}{\partial x}\right) + \frac{\partial u_c}{\partial z} \\ &\gamma_{yz}^c = 2\varepsilon_{yz}^c = \left(\frac{\partial w_c}{\partial y}\right) + \frac{\partial v_c}{\partial z} \end{aligned} \tag{5}$$

2.2. Compatibility Conditions

Assuming perfect bonding between the top and bottom face sheet-core interfaces, the compatibility. conditions are as shown below:

$$\begin{aligned} &u_c(z = z_{ci}) = u_0^i + \frac{1}{2}(-1)^k h_i \phi_x^i \\ &v_c(z = z_{ci}) = v_0^i + \frac{1}{2}(-1)^k h_i \phi_y^i \\ &w_c(z = z_{ci}) = w_0^i \\ &i = t \to k = 1\,;\; z_{ct} = \frac{h_c}{2} \\ &i = b \to k = 0\,;\; z_{cb} = -\frac{h_c}{2} \end{aligned} \tag{6}$$

By replacing Eqs. (4) and (6) in Eq. (5) and some simplification, the compatibility conditions are transformed into (7):

$$\begin{aligned} u_2^c &= \frac{[2(u_0^t + u_0^b) - h_t\phi_x^t + h_b\phi_x^b - 4u_0^c]}{h_c^2} \\ u_3^c &= \frac{\begin{bmatrix} 4(u_0^t + u_0^b) - 2(h_t\phi_x^t + h_b\phi_x^b) \\ -4h_c u_1^c - 4h_c u_0^c/R_{xc} \end{bmatrix}}{h_c^3} \\ v_2^c &= \frac{[2(v_0^t + v_0^b) - h_t\phi_y^t + h_b\phi_y^b - 4v_0^c]}{h_c^2} \\ v_3^c &= \frac{\begin{bmatrix} 4(v_0^t + v_0^b) - 2\left(h_t\phi_y^t + h_b\phi_y^b\right) \\ -4h_c v_1^c - 4h_c v_0^c/R_{yc} \end{bmatrix}}{h_c^3} \\ w_1^c &= \frac{[2(w_0^t + w_0^b)]}{h_c^2} \\ w_2^c &= \frac{[2(w_0^t + w_0^b) - 4w_0^c]}{h_c^2} \end{aligned} \tag{7}$$

According to Eq. (7), it is observed that the number of unknowns in the core layer is reduced to five, which are:: $u_1^c, u_0^c, v_0^c, v_1^c, w_0^c$. Thus, in general, all the unknowns for a flat composite sandwich panel are 15, which are [27]:

$$u_0^t, v_0^t, w_0^t, \phi_x^t, \phi_y^t, u_0^b, v_0^b, w_0^b, \phi_x^b, \phi_y^b, u_0^c, u_1^c, v_0^c, v_1^c, w_0^c \quad (8)$$

2.3. Relationships between stresses, resulting stresses, and moments of inertia of the core and face sheet

As mentioned, there is no normal stress in the ER layer, and only transverse shear stresses are:

$$\begin{aligned}&\sigma_{xz}^c = G_{2b(xz)}^C \gamma_{xz}^c = \\ &G_{2b(xz)}^C\left[w_{0,x}^c + zw_{1,x}^c + z^2 w_{2,x}^c\right] \\ &+G_{2b(xz)}^C[u_1^c + 2zu_2^c + 3z^2 u_3^c] \\ &\sigma_{yz}^c = G_{2b(yz)}^C \gamma_{yz}^c = \\ &G_{2b(yz)}^C\left[w_{0,y}^c + zw_{1,y}^c + z^2 w_{2,y}^c\right] \\ &+G_{2b(yz)}^C[v_1^c + 2zv_2^c + 3z^2 v_3^c]\end{aligned} \quad (9)$$

In this article, the modified Yalcinatas model [28] will be used as follows:

$$\begin{aligned}&G_{2b(xz)}^C = G_{b(xz)}^{'C} + G_{b(xz)}^{''C} \\ &G_{2b(yz)}^C = G_{b(yz)}^{'C} + G_{b(yz)}^{''C} \\ &G_{b(xz)}^{'C} = G_{b(yz)}^{'C} = 50.000E^2 \\ &G_{b(xz)}^{''C} = G_{b(yz)}^{''C} = 2600\,E + 1700\end{aligned} \quad (10)$$

where $G_{b(xz)}^{'C}$ is the coefficient of shear reserve, and $G_{b(xz)}^{''C}$ is Wasting factor.

The effect of the electric field on the vibration response of the ER sandwich plate can be seen for electric field levels of 0, 1, 2, and 3.5 kV/mm, respectively. Following [29], the results of the stress for the core can be written as follows:

$$\begin{aligned}&\begin{Bmatrix} N_{xx}^c \\ N_{yy}^c \\ N_{xy}^c \end{Bmatrix} = \int_{-h_c/2}^{h_c/2} \begin{Bmatrix} \sigma_{xx}^c \\ \sigma_{yy}^c \\ \sigma_{xy}^c \end{Bmatrix} dz_c \\ &\begin{Bmatrix} M_{nxx}^c \\ M_{nyy}^c \\ M_{nxy}^c \end{Bmatrix} = \int_{-h_c/2}^{h_c/2} z_c^n \begin{Bmatrix} \sigma_{xx}^c \\ \sigma_{yy}^c \\ \sigma_{xy}^c \end{Bmatrix} dz_c \\ &\begin{Bmatrix} N_{xz}^c \\ N_{yz}^c \\ M_{nxz}^c \\ M_{nyz}^c \end{Bmatrix} = \int_{-h_c/2}^{h_c/2} z_c^n \begin{Bmatrix} \sigma_{xz}^c \\ \sigma_{yz}^c \\ z_c^n \sigma_{xz}^c \\ z_c^n \sigma_{yz}^c \end{Bmatrix} dz_c \\ &\{R_z^c, M_z^c\} \\ &= \int_{-h_c/2}^{h_c/2} (1, z_c)\sigma_{zz}^c dz_c \ , \qquad n \\ &= 1,2,3\end{aligned} \quad (11)$$

If the face sheet is made of several orthotropic layers with different angles of rotation relative to the original coordinates, Relation (11) expresses the stress of the k[th] layer [30].

$$\begin{aligned}&\begin{bmatrix} \sigma_{xx} \\ \sigma_{yy} \\ \sigma_{xy} \end{bmatrix} = \begin{bmatrix} \bar{Q}_{11} & \bar{Q}_{12} & \bar{Q}_{16} \\ \bar{Q}_{12} & \bar{Q}_{22} & \bar{Q}_{26} \\ \bar{Q}_{16} & \bar{Q}_{26} & \bar{Q}_{66} \end{bmatrix}^{(k)} \begin{bmatrix} \varepsilon_{xx} \\ \varepsilon_{yy} \\ \varepsilon_{xy} \end{bmatrix} \\ &\begin{bmatrix} \sigma_{yz} \\ \sigma_{xz} \end{bmatrix} = \begin{bmatrix} \bar{Q}_{44} & \bar{Q}_{45} \\ \bar{Q}_{45} & \bar{Q}_{55} \end{bmatrix}^{(k)} \begin{bmatrix} \varepsilon_{yz} \\ \varepsilon_{xz} \end{bmatrix}\end{aligned} \quad (12)$$

where $\bar{Q}_{ij}$ denotes the transmitted stiffness. The relationship between axial stiffness and the transferred stiffness is given by Relation (13):

$$\{\bar{Q}_{ij}\}_k = [TM]_k \{Q_{ij}\}_k \quad (13)$$

where $[TM]_k$ is the stiffness matrix of the axial-to-axial unidirectional composite.

$$\begin{aligned}&Q_{11} = \frac{E_1}{1 - v_{12}v_{21}}, Q_{12} = \frac{v_{12}E_1}{1 - v_{12}v_{21}} \\ &Q_{22} = \frac{E_2}{1 - v_{12}v_{21}} \\ &Q_{66} = G_{12}, \ \ Q_{44} = G_{23}, \ \ Q_{55} = G_{13}.\end{aligned} \quad (14)$$

$Q_{ij}^{(k)}$ is the multilayer rigidity in the main axis of the material, and $\bar{Q}_{ij}$ denotes the rigidity transmitted in the geometric axis of the sandwich panel.

$$\begin{aligned}&\bar{Q}_{11} = Q_{11}\cos^4\theta + 2(Q_{12} \\ &\qquad + 2Q_{66})\sin^2\theta\cos^2\theta \\ &+\bar{Q}_{22}\sin^4\theta \\ &\bar{Q}_{12} = (Q_{11} + Q_{22} - 4Q_{66})\sin^2\theta\cos^2\theta \\ &+Q_{12}(\sin^4\theta + \cos^4\theta) \\ &\bar{Q}_{22} = Q_{11}\sin^4\theta + 2(Q_{12} \\ &\qquad + 2Q_{66})\sin^2\theta\cos^2\theta \\ &+\bar{Q}_{22}\cos^4\theta \\ &\bar{Q}_{16} = (Q_{11} - Q_{12} - 2Q_{66})\sin\theta\cos^3\theta \\ &+(Q_{12} - Q_{22} + 2Q_{66})\sin^3\theta\cos\theta \\ &\bar{Q}_{26} = (Q_{11} - Q_{12} - 2Q_{66})\sin^3\theta\cos\theta \\ &+(Q_{12} - Q_{22} + 2Q_{66})\sin\theta\cos^3\theta \\ &\bar{Q}_{66} = (Q_{11} + Q_{22} - 2Q_{12} \\ &\qquad - 2Q_{66})\sin^2\theta\cos^2\theta \\ &+Q_{66}(\sin^4\theta + \cos^4\theta) \\ &\bar{Q}_{44} = Q_{44}\cos^4\theta + Q_{55}\sin^4 \\ &\bar{Q}_{45} = (Q_{55} - Q_{44})\cos\theta\sin\theta \\ &\bar{Q}_{55} = Q_{55}\cos^4\theta + Q_{44}\sin^4\theta\end{aligned} \quad (15)$$

The basic multi-layer relationships of the face sheet are derived from the following relationship:

$$\begin{aligned}&N_{xx}^i = A_{11}^i u_{,x}^i + A_{12}^i v_{,y}^i + A_{16}^i\left(u_{,y}^i + v_{,x}^i\right) \\ &+B_{12}^i \phi_{y,y}^i + B_{16}^i\left(\phi_{x,y+}^i \phi_{y,x}^i\right) \\ &N_{yy}^i = A_{12}^i u_{,x}^i + A_{22}^i v_{,y}^i + A_{26}^i\left(u_{,y}^i + v_{,x}^i\right) \\ &+B_{12}^i \phi_{x,x}^i + B_{22}^i \phi_{y,y}^i + B_{26}^i\left(\phi_{x,y+}^i \phi_{y,x}^i\right) \\ &N_{xy}^i = A_{16}^i u_{,x}^i + A_{26}^i v_{,y}^i + A_{66}^i\left(u_{,y}^i + v_{,x}^i\right) \\ &\quad +B_{16}^i \phi_{x,x}^i + B_{26}^i \phi_{y,y}^i + B_{66}^i\left(\phi_{x,y+}^i \phi_{y,x}^i\right) \\ &M_{xx}^i = B_{11}^i u_{,x}^i + B_{12}^i v_{,y}^i + B_{16}^i\left(u_{,y}^i + v_{,x}^i\right) \\ &+D_{11}^i \phi_{x,x}^i + D_{12}^i \phi_{y,y}^i + D_{16}^i\left(\phi_{x,y+}^i \phi_{y,x}^i\right) \\ &M_{yy}^i = B_{12}^i u_{,x}^i + B_{22}^i v_{,y}^i + B_{26}^i\left(u_{,y}^i + v_{,x}^i\right) \\ &+D_{12}^i \phi_{x,x}^i + D_{22}^i \phi_{y,y}^i + D_{26}^i\left(\phi_{x,y+}^i \phi_{y,x}^i\right) \\ &M_{xy}^i = B_{16}^i u_{,x}^i + B_{26}^i v_{,y}^i + B_{66}^i\left(u_{,y}^i + v_{,x}^i\right) \\ &+D_{16}^i \phi_{x,x}^i + D_{26}^i \phi_{y,y}^i + D_{66}^i\left(\phi_{x,y+}^i \phi_{y,x}^i\right)\end{aligned} \quad (16)$$

$$Q_{yz}^{i} = k\left[A_{44}^{i}\left(\phi_{y}^{i} + w_{,y}^{i}\right) + A_{45}^{i}\left(\phi_{x}^{i} + w_{,x}^{i}\right)\right]$$
$$Q_{xz}^{i} = k\left[A_{45}^{i}\left(\phi_{y}^{i} + w_{,y}^{i}\right) + A_{55}^{i}\left(\phi_{x}^{i} + w_{,x}^{i}\right)\right]$$

The stiffness coefficients are defined as follows:

$$\left(A_{ij}, B_{ij}, D_{ij}\right)^{m} = \int_{-h_m/2}^{h_m/2} \overline{Q}_{ij}\left(1, z, z^2\right) dz_m \quad (17)$$
$$= \left(\sum_{k=1}^{N} \overline{Q}_{ij}^{(k)} \int_{z_{(k)}}^{z_{(k+1)}} (1, z, z^2) dz\right)^{m}$$
$$A_{ij}^{m} = \left(\sum_{k=1}^{N} \overline{Q}_{ij}^{(k)} \left(z_{(k+1)} - z_{(k)}\right)\right)^{m}$$
$$B_{ij}^{m} = \left(\frac{1}{2}\sum_{k=1}^{N} \overline{Q}_{ij}^{(k)} \left(z_{(k+1)}^2 - z_{(k)}^2\right)\right)^{m}$$
$$D_{ij}^{m} = \left(\frac{1}{3}\sum_{k=1}^{N} \overline{Q}_{ij}^{(k)} \left(z_{(k+1)}^3 - z_{(k)}^3\right)\right)^{m} \quad i, j = 1,2,6 \; ; \; m = t, b$$
$$A_{ij}^{m} = \left(\sum_{k=1}^{N} \overline{Q}_{ij}^{(k)} \left(z_{(k+1)} - z_{(k)}\right)\right)^{m} \quad i, j = 4,5 \; ; \; m = t, b$$

The following integrals are defined to express the equations of motion in terms of displacement and to facilitate the process of solving equations:

$$e_n^{c(xx)} = \int_{-\frac{h_c}{2}}^{\frac{h_c}{2}} Z_c E_{xx}^{C}(Z)\, dz \quad n = 0.1.2.3 \quad (18)$$
$$e_n^{c(yy)} = \int_{-\frac{h_c}{2}}^{\frac{h_c}{2}} Z_c E_{yy}^{C}(Z)\, dz \quad n = 0.1.2.3$$
$$g_n^{c(xy)} = \int_{-\frac{h_c}{2}}^{\frac{h_c}{2}} Z_c^n G_{xy}^{C}(Z)\, dz \quad n = 0.1.2.3$$
$$g_n^{c(xz)} = \int_{-\frac{h_c}{2}}^{\frac{h_c}{2}} Z_c^n G_{(xz)}^{C}(Z)\, dz \quad n = 0.1.2.3$$

The moment of inertia of the core is as follows:

$$I_n^c = \int_{-\frac{h_c}{2}}^{\frac{h_c}{2}} \rho_c z_c^n\, dz_c \quad n = 0,1, \ldots, 6 \quad (19)$$

Also, the moment of inertia of the face sheets in the relation is:

$$I_n^i = \int_{-\frac{h_i}{2}}^{\frac{h_i}{2}} z_i^n\, \rho_i dz_i, \; i = t, b \quad (20)$$

Stress resultants per unit length for top and bottom face sheets can be defined as follows:

$$\begin{Bmatrix} N_{xx}^{i} \\ N_{yy}^{i} \\ N_{xy}^{i} \end{Bmatrix} = \int_{-h_i/2}^{h_i/2} \begin{Bmatrix} \sigma_{xx}^{i} \\ \sigma_{yy}^{i} \\ \sigma_{xy}^{i} \end{Bmatrix} dz_i \quad (21)$$
$$\begin{Bmatrix} M_{xx}^{i} \\ M_{yy}^{i} \\ M_{xy}^{i} \end{Bmatrix} = \int_{-h_i/2}^{h_i/2} \begin{Bmatrix} \sigma_{xx}^{i} \\ \sigma_{yy}^{i} \\ \sigma_{xy}^{i} \end{Bmatrix} dz_i$$
$$\begin{Bmatrix} Q_{xz}^{i} \\ Q_{yz}^{i} \end{Bmatrix} = k_s \int_{-h_i/2}^{h_i/2} \begin{Bmatrix} \sigma_{xz}^{i} \\ \sigma_{yz}^{i} \end{Bmatrix} dz_i, \quad i = t, b$$

where k_s is shear correction factor.

2.4. Applying the Hamiltonian principle

To obtain the equations governing motion, we use the Hamiltonian [20] principle, which states:

$$\int_0^t \delta L dt = \int_0^t (\delta K - \delta U + \delta W_{ext}) dt = 0. \quad (22)$$

where δK represents the kinetic energy variations, δU denotes the potential energy variations, and δW_{ext} shows the energy variations caused by the forces on the problem. Here, for studying free vibrations, the dynamically distributed vertical loads on the upper surface of q_t and q_b are defined as zero.

$$\delta W_{ext} = \int_A \left(-q_t \delta w_0^t + q_b \delta w_0^b\right) dx\, dy \quad (23)$$

Assuming homogeneous conditions for displacement and velocity for the time coordinate for a sandwich plate, the kinetic and potential energies variations can be generalized as:

$$\delta K = -\sum_{i=t,b,c}\left[\iint_{A_i}\int_{-h_i/2}^{h_i/2} \rho_i \begin{pmatrix} \ddot{u}_i \delta u_i \\ +\ddot{v}_i \delta v_i + \\ \ddot{w}_i \delta w_i \end{pmatrix} dz_i\, dA_i\right] \quad (24)$$
$$dA_c = dx_c dy_c$$
$$dA_i = dx_i dy_i, \quad (i = t, b)$$
$$\delta U = \sum_{i=t,b}\left(\int_{V_i}\begin{pmatrix} \sigma_{xx}^{i}\delta\varepsilon_{xx}^{i} + \\ \sigma_{yy}^{i}\delta\varepsilon_{yy}^{i} + \\ \tau_{xz}^{i}\delta\gamma_{xz}^{i} + \\ \tau_{xy}^{t}\delta\gamma_{xy}^{i} \\ +\tau_{yz}^{i}\delta\gamma_{yz}^{i} \end{pmatrix} dV_i\right) \quad (25)$$
$$+ \int_{V_c}\begin{pmatrix} \sigma_{xx}^{c}\delta\varepsilon_{xx}^{c} + \sigma_{yy}^{c}\delta\varepsilon_{yy}^{c} \\ +\sigma_{zz}^{c}\delta\varepsilon_{zz}^{c} \\ +\tau_{xy}^{c}\delta\gamma_{xy}^{c} \\ +\tau_{xz}^{c}\delta\gamma_{xz}^{c} + \tau_{yz}^{c}\delta\gamma_{yz}^{c} \end{pmatrix} dV_c$$
$$dV_c = dA_c dZ_c = dx_c dy_c dz_c$$
$$dV_i = dA_i dz_i = dx_i dy_i dz_i \; ; \; (i = t, b)$$

Finally, the 15 equations of motion for the flat sandwich plate with the ER core are obtained using the Hamiltonian principle. Given the long equations, only one equation is given as an example:

$$\delta W_0^C: \quad \frac{4M_{2xx}^{c}}{R_{xc}h_c^2} + \frac{\partial N_{xz}^{c}}{\partial x} - \frac{4}{h_c^2}\frac{\partial M_{2xz}^{c}}{\partial x} - \frac{4}{h_c^2}\frac{\partial M_{2yz}^{c}}{\partial y} \quad (26)$$

$$+\frac{\partial N_{yz}^{c}}{\partial y}+\frac{8}{h_c^2}M_z^c=\left(\frac{16I_4^c}{h_c^4}-\frac{8I_2^c}{h_c^2}+I_0^c\right)\ddot{W}_0^c+\left(\frac{2I_2^c}{h_c^2}-\frac{8I_4^c}{h_c^4}+\frac{I_1^c}{h_c}-\frac{4I_3^c}{h_c^3}\right)\ddot{W}_0^t+\left(\frac{2I_2^c}{h_c^2}-\frac{8I_4^c}{h_c^4}-\frac{I_1^c}{h_c}+\frac{4I_3^c}{h_c^3}\right)\ddot{W}_0^b$$

Displacement fields based on the double Fourier series for a flat composite sandwich panel with a simply supported boundary condition at the top and bottom face sheets are assumed to be in the following form (i = t,b) [32]:

$$\begin{bmatrix} u_0^j(x,y,t)\\ v_0^j(x,y,t)\\ w_0^j(x,y,t)\\ \phi_x^j(x,y,t)\\ \phi_y^j(x,y,t)\\ u_k^c(x,y,t)\\ v_k^c(x,y,t)\\ w_l^c(x,y,t)\end{bmatrix} = \sum_{n=1}^{\infty}\sum_{m=1}^{\infty}\begin{bmatrix} U_{0mn}^j\cos(\alpha_m x)\sin(\beta_n y)\\ V_{0mn}^j\sin(\alpha_m x)\cos(\beta_n y)\\ W_{0mn}^j\sin(\alpha_m x)\sin(\beta_n y)\\ \phi_{xmn}^j\cos(\alpha_m x)\sin(\beta_n y)\\ \phi_{ymn}^j\sin(\alpha_m x)\mathrm{coc}(\beta_n y)\\ U_{kmn}^c\cos(\alpha_m x)\sin(\beta_n y)\\ V_{kmn}^c\sin(\alpha_m x)\cos(\beta_n y)\\ W_{lmn}^j\sin(\alpha_m x)\sin(\beta_n y)\end{bmatrix} e^{i\omega t} \quad (27)$$

$(k = 0,1,2,3), (l = 0,1,2)$

Where $\alpha_m = \frac{m\pi}{a}$ *and* $\beta_n = \frac{n\pi}{b}$.

When all edges are clamped, functions $\cos(\alpha_m x)$ and $\cos(\beta_n y)$ in the above series expansions must be replaced with $\sin(\alpha_m x)$ and $\sin(\beta_n y)$, respectively.

In Eq.(27), U_{0mn}^j, V_{0mn}^j, W_{0mn}^j, ϕ_{xmn}^j, ϕ_{ymn}^j, U_{kmn}^c, V_{kmn}^c and W_{lmn}^j are the Fourier coefficients, and m and n are half wavenumbers along x and y directions, respectively. By substituting stress resultants (Eq. (27)), compatibility conditions (Eq. (7)), and displacement field (Eq. (30)) in the governing equations (Eqs. (11)-(25)), applying the Galerkin method, and collecting coefficients, the eigenvalue equation is obtained as follows:

$$[M]\{\ddot{c}\}+[K]\{c\}=\{0\} \quad (28)$$
$$\{c\}=\{U_{0mn}^t, U_{0mn}^b, V_{0mn}^t, V_{0mn}^b, W_{0mn}^t, \cdots W_{0mn}^b, \phi_{xmn}^t, \psi_{xmn}^b, \phi_{ymn}^t \psi_{ymn}^b, \cdots U_{0mn}^c, V_{0mn}^c, u_{1mn}^c, V_{0mn}^c, W_{0mn}^c\}^t$$

Hence, the problem of free vibration of the sandwich plate with simple support becomes the standard equation of structural response; [K] represents stiffness matrices, and [M] represents matrices of mass. Finally, by assuming free vibrations, one can calculate the natural frequencies, ω, and modal damping coefficients η_v for different vibrational modes from Eq (29): [22-24]:

$$\omega=\sqrt{Re(\tilde{\omega}^2)},\quad \eta_v=\frac{Im(\tilde{\omega}^2)}{Re(\tilde{\omega}^2)} \quad (29)$$

3. Results and Discussion

3.1. Validation of Equations

Here are two examples (Example 1: Flat sandwich plate with an aluminum case and MR intelligent oil core and Example 2: Flat sandwich plate with an aluminum face sheet and ER smart liquid core) of the structure and the results are discussed. To verify the equations obtained, the results obtained in the present work are compared with a recent study and definitely with the MR core. Then, the results obtained with the ER core are reviewed.

The mechanical and geometrical properties of the structure considered in example 1 are presented in Table 1. The upper and lower portions of the pure aluminum are [0,0,0], and the sheet is symmetrical to the middle plate.

Table 2 presents the results of the current study for a flat sandwich panel with MR core using the improved high-order theory of sandwich panel, it further compared the results with those obtained from the classical theory of multilayer sheets [33]. Kirchhoff's theory is used for the face sheets [33]. Table 4 presents the results of this study for a flat sandwich panel with ER core. In Table 2 using the improved high-order theory of sandwich panel, compared with the findings of the classical theory of multilayer Sheets [34].

3.2. Free vibration analysis

In this section, the free vibrations of a composite sandwich panel and ER core are investigated. The effects of changing the thickness of the ER layer and the electric field intensity are also examined on the natural frequencies of the sheet. The lay-up sequences for face sheets were [0/0/0/core/0/0/0], and the sandwich panel was symmetric around the mid-plane. Mechanical and geometrical properties of the flat sandwich panel with an aluminum face sheet and ER core are presented in Table 3.

Table 1. Mechanical and geometrical properties of the flat sandwich panel with aluminum face sheet and MR core [33]

Geometry	Face sheet	Core
a=0.4m	E1=E2=E3=70GPa	ρ =3500Kg/m3
b=0.4m	G12=G13= G23=26.9 GPa	G13 = G23= $G = G' + iG''$
h_c=0.5mm	v = 0.3	G'= -3.3691B2+4.9975×103B +0.873×106
ht=hb=0.5 mm	ρ =2700 Kg/m3	G''=-0.9B2+0.8124×103B +0.1855×106

Table 2. Natural frequency values, first to fourth, for the flat sandwich panel with an aluminum face sheet and MR core. The lay-up sequences for face sheets were [0 / core / 0] and B = 0, a / b = 1, h_c / h_t = 4.

Mode	Natural frequency (Hz) Present model	modal factor Present model	Natural frequency (Hz) Reference [30]	modal factor Reference [33]	Error difference for Natural frequency (%) Present model and reference [33]
1	28.5629	0.1642	28.0081	0.1062	2.007
2	49.671	0.1652	48.6992	0.1243	1.996
3	49.671	0.1652	48.6992	0.1243	1.996
4	66.4289	0.1556	65.2157	0.1204	1.860

Table 3. Mechanical and geometrical properties of flat sandwich sheets with an aluminum face sheet and ER core [34]

Geometry	Face sheet	Core
a=0.4m	E1=E2=E3=70 GPa	ρ =1700 Kg/m3
b=0.4m	G12=G13= G23=26.9 GPa	$G^{C}_{2b(xz)} = G^{'C}_{b(xz)} + G^{'C}_{b(xz)}$ $G^{C}_{2b(yz)} = G^{'C}_{b(yz)} + G^{''C}_{b(yz)}$
h_c=0.5mm	v = 0.3	$G^{'C}_{b(xz)} = G^{'C}_{b(yz)} = 50000E^2$
ht=hb=0.5 mm	ρ =2700 Kg/m3	$G^{''C}_{b(xz)} = G^{''C}_{b(yz)} = 2600\,E + 1700$

Table 4: Normal frequency values, first to fourth, for the flat sandwich panel with an aluminum face sheet and ER core. The lay-up sequences for E=0, a/b=1, /h_c / h_t =1 sheets were [0/core/0]

Mode	Natural frequency (Hz) Present model	modal factor Present model	Natural frequency (Hz) Reference [31]	modal factor Reference [34]	Error difference for Natural frequency (%) Present model and reference [34]
1	31.193	0.01719	31.1952	0.0172	0.007
2	32.9808	0.0068	32.9808	0.0069	0
3	32.9808	0.0068	32.9808	0.0069	0
4	52.7685	0.0042	52.7693	0.0043	0.002

Kirchhoff's theory was used in the face sheet for reference [34]. Table 5 displays the the first natural frequency and the corresponding modal loss factor for the first few mode numbers (m,n = 1,2), selected ER core layer thickness parameters (h_c / h_t = 1,4), geometric aspect ratios (a/b = 1,2,4), and electric field strengths (E =0,1,2,3.5 kVmm−1).

The most important observations are as follows. The natural frequencies increase with increasing the electric field strength and/or the geometric aspect ratio. In particular, the effect of increasing electric field strength is more evident on the natural frequencies associated with lower mode numbers in comparison with those of the higher modes.

The natural frequencies decrease with increasing ER core layer thickness. On the other hand, increasing the electric field strength appears to have different effects on the modal loss factors, depending on the geometric aspect ratio.

3.2.1 Natural frequency of flat sandwich plate with ER core

Fig. 2 illustrates the comparison of the frequencies obtained with different electric fields.

The natural frequencies of the sandwich plate with different electric fields are shown in Fig. 2. The effect of the electric field on the vibration response of the ER sandwich plate can be seen for electric field levels of 0, 1, 2, and 3.5 kV/mm. It can be seen that higher electric field strength increases the natural frequencies of the sandwich plate.

Fig. 3 compares the damping coefficient in terms of vibrational modes and different electric fields. Fig. 3 shows the variations in the modal loss factor as a function of electric field. It can be seen that the modal loss factor decreases as the electric field increases. Also, a relative decrease in the modal loss factor can be observed with increasing mode number.

3.2.2 Influence of the ratio of core thickness to total sheet thickness on the first natural frequency

The thickness of the core has an important effect on the vibration of the sheet. Fig. 4 reveals the diagram of the first frequency changes of the flat sandwich plate with an ER core in terms of different core thickness to plate thickness (h_c / h) ratios for different electric field intensities (KV / mm) at a = b.

It is observed from Fig. 4 that by increasing the ratio of core thickness up to total sheet thickness, the natural frequency of the sheet diminishes. Since the core is made of oil and composite surfaces, the core modulus is smaller than the surface. Also, as the core thickness-to-whole ratio increases, the overall sheet modulus drops. As a result, the natural frequency of the sheet is also reduced.

Table 5: First-fourth frequency values and modal damping coefficients for the first four vibration modes for core thickness, field intensity, and different aspect ratio of the flat sandwich panel with aluminum face sheets and an ER core

Mode	h_c / h_t		E=0 KV/mm		E=1 KV/mm		E=2 KV/mm		E=3.5 KV/mm	
		a/b	$\omega(Hz)$	η_v	$\omega(Hz)$	η_v	$\omega(Hz)$	η_v	$\omega(Hz)$	η_v
(1,1)	1	1	13.191	0.0172	16.0786	0.0269	21.8029	0.0187	29.7509	0.0093
		2	32.9776	0.0068	36.111	0.0140	43.7297	0.0139	57.636	0.0098
		4	112.126	0.0020	115.399	0.0047	124.527	0.0064	145.646	0.0067
	4	1	10.0634	0.0268	13.4363	0.0373	20.2129	0.0248	31.1408	0.0139
		2	25.1577	0.0107	28.8489	0.0205	37.6856	0.0188	54.443	0.0131
		4	85.5375	0.0031	89.4219	0.0072	100.124	0.0092	124.606	0.0091
(1,2)	1	1	32.9776	0.0068	36.1111	0.0140	43.7297	0.0139	57.636	0.0098
		2	52.7606	0.0043	5596.59	0.0094	64.3059	0.0108	81.2639	0.0090
		4	131.904	0.0017	135.186	0.0041	144.434	0.0056	166.288	0.0062
	4	1	25.1577	0.0107	28.8489	0.0205	37.6856	0.0188	54.443	0.0131
		2	40.2495	0.0067	44.0391	0.0141	53.7357	0.0149	73.6189	0.0119
		4	100.625	0.0026	104.523	0.0062	115.386	0.0082		0.0085
(2,1)	1	1	32.9776	0.0068	36.1111	0.0140	43.7297	0.0139	57.636	0.0098
		2	112.126	0.0020	115.399	0.0047	124.527	0.0064	145.646	0.0067
		4	428.669	0.0005	431.988	0.0013	441.744	0.0020	467.165	0.0027
	4	1	428.669	0.0005	431.988	0.0013	441.744	0.0020	467.165	0.0027
		2	85.5375	0.0031	89.4219	0.0072	100.124	0.0092	124.606	0.0091
		4	327.018	0.0008	330.97	0.0020	342.537	0.0030	372.394	0.0040
(2,2)	1	1	52.7606	0.0043	55.9659	0.0094	64.3059	0.0108	81.2639	0.0090
		2	131.904	0.0017	135.186	0.0041	144.434	0.0056	166.288	0.0062
		4	448.44	0.0005	451.759	0.0012	461.526	0.0019	487.031	0.0026
	4	1	40.2495	0.0067	44.0391	0.0144	53.7355	0.0149	73.6189	0.0119
		2	100.625	0.0026	104.523	0.0062	115.386	0.0082	140.733	0.0085
		4	342.1	0.0007	346.053	0.0019	357.636	0.0029	387.607	0.0038

The oil density is also high, and as the amount of oil increases, the sheet becomes significantly heavier-hence the stiffness-to-mass ratio falls, resulting in a decline in the natural frequency of the sheet.

3.2.3 Influence of fiber angle on the natural frequency

Fig. 5 displays the diagram of the natural frequency changes of the first flat sandwich plate with an ER core in terms of the lay-up sequences for face sheets. From Fig. 5, it is observed that the maximum level of the natural frequency occurs in a state θ equal to 45 degrees, as in this case the flexural stiffness has its maximum value. Also, with increasing electric field strength in higher modes, natural frequencies increase as well.

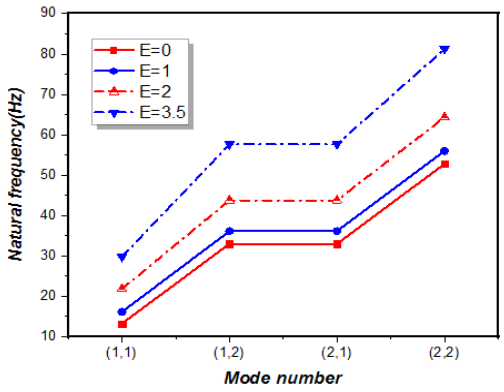

Fig. 2. Diagram of changes in the natural frequency of the sheet for different electric field intensities

3.2.4. Influence of electric field intensity on the natural frequency

Fig. 6 reveals the diagram of the first natural frequency variations of the flat sandwich plate with an ER core in terms of electric field intensity for different aspect ratios.

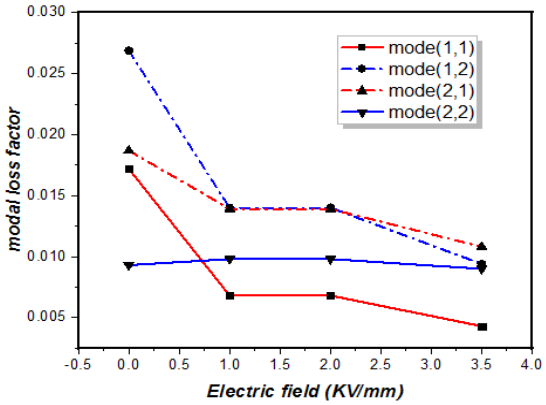

Fig. 3. Diagram of changes in the damping coefficients in the first four vibrational modes for different electric field intensities

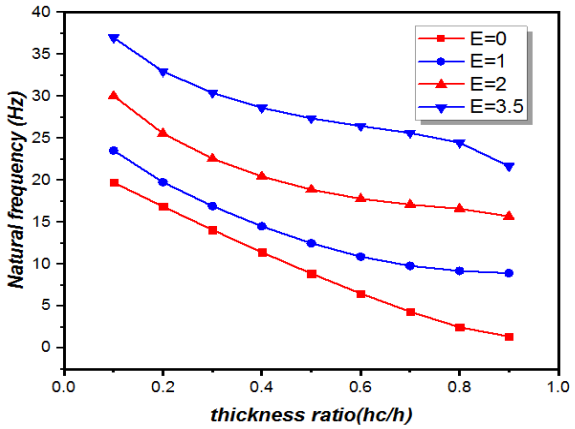

Fig. 4. Diagram of the first frequency changes of the sheet in different ratios of the core to sheet thickness for different electric field intensities

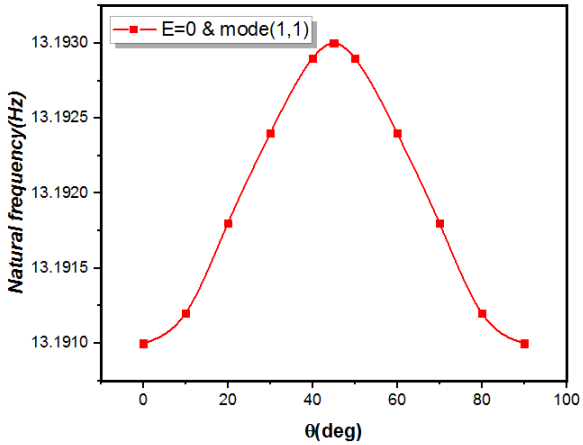

(a)

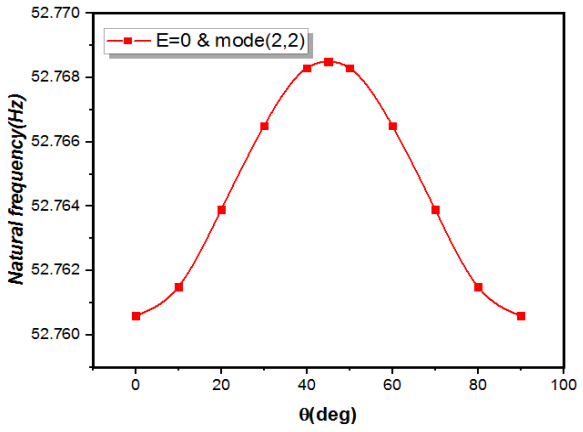

(b)

Fig. 5. (a) Diagram of the first frequency changes of the sheet in terms of the different fiber orientations layer of the composite face sheet and (b) diagram of the fourth frequency changes of the sheet in terms of the different fiber orientations layer of the composite face sheet

Fig. 6 shows that the natural frequency of the sheet increases with increasing the intensity of the electric field. It is because, according to (9) and (10), as the electric field increases, so does the structural stiffness, and thus the natural frequency is also enhanced.

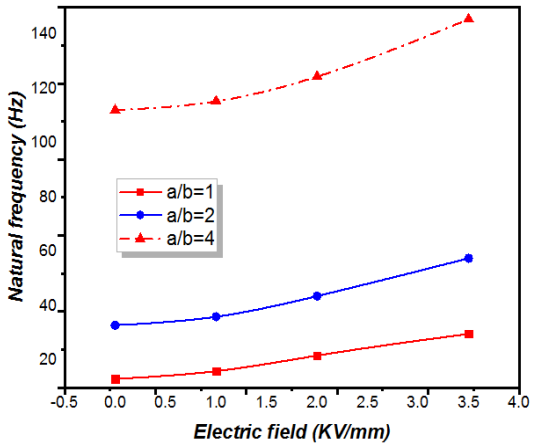

Fig. 6. Diagram of the first frequency change of the sheet in terms of electric field intensity for different aspect ratios

However, this rise in frequency only proceeds partly from the increase in the electric field intensity and does not grow from one value to the next. Also, it is almost proved to be saturated as the intensity of the electric field, which is approximately 3.5 kV /mm in this study.

3.2.5. The effect of aspect ratio on the natural frequency

Figure 7 reveals the diagram of the first natural frequency variations of the flat sandwich plate with an ER core in terms of the aspect ratio for the intensity of different electric fields. According to Fig. 7, it is observed that with increasing the aspect ratio, the natural frequency of the sheet increases. With the rise of the aspect ratio, the sheet gradually becomes a beam with enhanced transverse stiffness and hence augmented natural frequency. By raising the intensity of the electric field from one point to the next, its effect on the natural frequency decreases. This is due to the saturation point; by increasing the intensity of the electric field, it saturates the oil at a given electric field intensity, after which increasing the field will not have much effect on increasing the rigidity and natural frequency of the sheet.

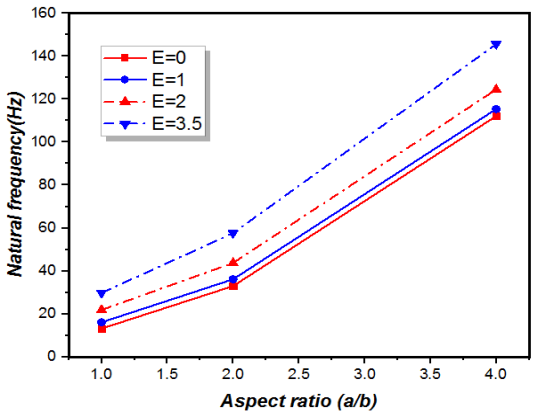

Fig. 7. Diagram of the first frequency changes of the sheet in terms of aspect ratio for different electric field intensities

3.2.6. Influence of length-to-thickness ratio on the natural frequency

Fig. 8 reveals the diagram of the natural frequency variations of the first flat sandwich plate with an ER core in terms of length to thickness ratio. According to Fig. 8 with increasing the length-to-thickness ratio, the natural frequency of the sheet decreases. As the ratio grows, the sheet becomes thinner and, as a result, its stiffness drops.

4. Conclusions

In this research, an extensive study was done on the modeling of a flat sandwich plate with an ER core. For the first time, the governing equations associated with the vibration behavior of a flat sandwich plate with a thick ER core were extracted. The obtained equations for the simply-supported boundary conditions discretized by the Galerkin method. Finally, the effects of different parameters on the vibrational characteristics of the sandwich plate with an ER layer were illustrated. Numerical results can be summarized as follows:

The generality of the problem indicates an increase in the natural frequencies of the sandwich plate owing to the existence of the ER. Thus, by creating an electric field whose intensity can be controlled, the natural frequencies and thus the vibrations of the structure can be controlled. According to the analytical results, the electric field will change the stiffness of the sandwich plate. As the applied electric field increases, the natural frequency of the sandwich plate increases too.

On the other hand, the modal loss factor of the sandwich plate plays an important role in the stability of the damped structures. It can be seen that the modal loss factor decreases as the electric field increases. Also, a relative decrease in the modal loss factor can be observed with increasing the mode number.

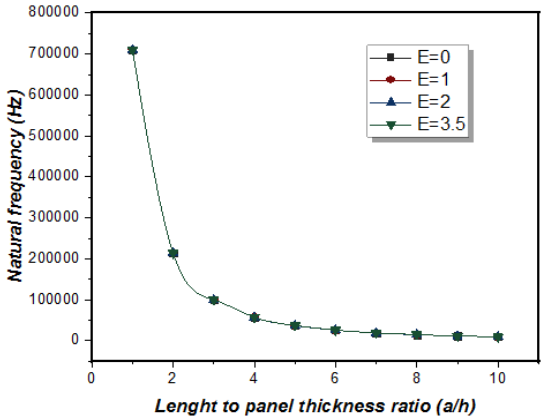

Fig. 8. Influence of length-to-thickness ratio on the natural frequency

The effect of the ER layer thickness on the core is such that by increasing the core thickness to sheet ratio for a constant electric field intensity, the frequency drops. Since the core is made of fluid and composite surfaces, the rigidity of the core is lower than that of the layer, and as a consequence, the overall rigidity decreases. Also, as the fluid content rises, the sheet becomes significantly heavier, and the stiffness-to-mass ratio diminishes.

The natural frequencies increase with increasing geometric aspect ratio, whereas they tend to decrease with increasing the ER core layer thickness. As the aspect ratio increases, the sheet gradually becomes a beam whose transverse stiffness grows, and thus the natural frequency increases.

By increasing the length-to-thickness ratio, the natural frequency of the sheet decreases. As this ratio grows, the sheet becomes thinner and, as a result, its stiffness declines. Thus, by changing this parameter, the natural frequency of the structure can also be obtained within the desired range. Finally, it is observed that applying an inappropriate electric field may significantly degrade the vibration control performance of the ERF-based plate, or even lead to maximum structural vibration levels. The effects of the sandwich structure with an ER core on the dynamic stability of plates and shells are also interesting topics to be studied.

Nomenclature

$I_n^i (i = t, b, c)$	The moments of inertia of the top and bottom face sheets and the core
M_z^c	Normal bending moments per unit length of the edge of the core
$M_{xy}^i, M_{xx}^i, M_{yy}^i$	Bending and shear moments per unit length of the edge (i=t,b)
$M_{nxx}^c, M_{nxy}^c, M_{ny}^c$ M_{nxz}^c, M_{nyz}^c	Shear and bending moments per unit length of the edge of the core,
$N_{xy}^i, N_{xx}^i, N_{yy}^i$	In-plane and shear forces per unit length of the edge (i=t,b)
N_{xz}^c, N_{yz}^c	The reduced-stiffness associated with the principal material coordinates
Q_{ij}	The reduced stiffnesses associated with the principal material coordinates
$\bar{Q}_{ij}$	Transformed reduced stiffnesses
u_k, v_k, w_k	Unknowns of the in-plane displacements of the core (k=0,1,2,3)
u_c, v_c, w_c	Displacement components of the core
u_0^i, v_0^i, w_0^i	Displacement components of the face sheets (i = t, b)
$\ddot{u}_c, \ddot{v}_c, \ddot{w}_c$	Acceleration components of the core

$\ddot{u}_{0i}, \ddot{v}_{0i}, \ddot{w}_{0i}$	Acceleration components of the face sheets, (i= t, b)
Z_t, Z_b, Z_c	Normal coordinates in the mid-plane of the top and the bottom face sheets and the core
dVt , dVc , dVb	Volume elements of the top face sheet, the core, and the bottom face sheet, respectively
Greek Letters	
ρ_t, ρ_b, ρ_c	Material densities of the face sheets and the core
σ_{ii}^{j}	Normal stress in the face sheets, (i=x,y), j=(t,b)
σ_{ii}^{c}	Normal stress in the core, (i=x,y,z)
$\tau_{xy}^{i}, \tau_{xz}^{j}, \tau_{yz}^{i}$	Shear stress in the face sheets, j=(t,b)
$\tau_{xy}^{c}, \tau_{xz}^{c}, \tau_{yz}^{c}$	Shear stresses in the core
$\varepsilon_{0xx}^{j}, \varepsilon_{0xy}^{j}, \varepsilon_{0yy}^{j}, \varepsilon_{0xz}^{j}, \varepsilon_{0xz}^{j}$	The mid-plane strain components, (i=t,b)
$\varepsilon_{zz}^{c}, \varepsilon_{xx}^{c}, \varepsilon_{yy}^{c}$	Normal strains components of the core layer
$\gamma_{xz}^{c}, \gamma_{yz}^{c}, \gamma_{xy}^{c}$	Shear strains components of the core layer
ϕ_x^i, ϕ_y^i	Rotation of the normal section of mid-surface of the top face sheet and the core bottom face sheet along x and y, respectively(i=t,b)

References

[1] Frostig, Y., Thomsen, O.T, 2004. Higher-order free vibration of sandwich panels with a flexible core. *International Journal of Solids and Structures*, 41(5), pp.1697–1724.

[2] Malekzadeh, K., Khalili, M.R., Mittal, R.K., 2005. Local and global damped vibrations of plates with a viscoelastic soft flexible core: an improved high-order approach. *Journal of Sandwich Structures and Materials*, 7(5), pp. 431-456.

[3] Reissner, E., 1945. The effect of transverse shear deformation on the bending of elastic plates. *ASME Journal of Applied Mechanics*, 12, pp. A68-A77.

[4] Mindlin, RD., 1951. Influence of rotatory inertia and shear on flexural motions of isotropic, elastic plates. *Journal of Applied Mechanics*, 18(1), pp. 31-38.

[5] Reddy J.N., 1984. A simple higher-order theory for laminated composite plates. *Journal of applied mechanics*, 51(4), pp. 745-52.

[6] Reddy, J.N., 2004. Mechanics of Laminated Composite Plates and Shells, Theory and Analysis. 2nd Edition, CRC Press, New York.

[7] Sayyad, A.S., Ghugal, Y.M., 2012. Bending and free vibration analysis of thick isotropic plates by using exponential shear deformation theory. *Applied and Computational Mechanics*, 6(1), pp. 65-82.

[8] Ghugal, Y.M., Sayyad, A.S., 2011. Free vibration of thick orthotropic plates using trigonometric shear deformation theory. *Latin American Journal of Solids and Structures*, 8(3), pp. 229-243.

[9] Ghasemi, A.R. and Mohandes, M., 2019. Free vibration analysis of rotating fiber-metal laminate circular cylindrical shells. *Journal of Sandwich Structures and Materials*, 21(3), pp. 1009–1031.

[10] Ghasemi, A.R., Taheri-Behrooz, F., Farahani, S.M.N, Mohandes, M., 2016. Nonlinear free vibration of a Euler-Bernoulli composite beam undergoing finite strain subjected different boundary conditions. *Journal of Vibration and Control*, 22(3), pp. 799–811.

[11] Payganeh, G., Malekzadeh, K., Malek-Mohammadi, H., 2016. Free Vibration of Sandwich Panels with Smart Magneto-Rheological Layers and Flexible Cores. *Journal of Solid Mechanics*, 8(1), pp. 12-30.

[12] Mozaffari, A., Karami, M. and Azarnia, A.H., 2013. The Effects of Embedded SMA Wires on Free Vibrations of Shape Memory Sandwich-Composite Panel. *Aerospace Mechanics Journal*, 44(2), pp. 29-40.

[13] Ghajar, R., Malekzadeh, K. and Gholami, M., 2015. Dynamic Response Analysis of Doubly Curved Composite Shells Subjected to Low-Velocity Impact Using Two Models of Complete and Improved Spring-Mass, *Aerospace Mechanics Journal*, 10(4), pp. 1-12

[14] Khorshidi, K., Siahpush, A., Fallah, A., 2107. Electro-Mechanical free vibrations analysis of composite rectangular piezoelectric nanoplate using modified shear deformation theories. *Journal of Science and Technology of Composites*, 4(2), pp. 151-160.

[15] Carlson, J.D., Coulter, J.P. and Duclos, T.G. ,1990. Electrorheological Fluid Composite Structures, US Patent 4,923,057.

[16] Don, D.L., 1993. An Investigation of Electrorheological Material Adaptive Structures, Master's Thesis, Lehigh University.

[17] Yalcintas, M. and Coulter, J.P., 1995. Analytical modelling of electrorheological material based adaptive beams. *Journal of Intelligent Material Systems and Structures*, 6(4), pp. 488-497.

[18] Sun, Q., Zhou, J.X. and Zhang, L. ,2003. An Adaptive Beam Model and Dynamic Characteristics of Magnetorheological Materials, *Journal of Sound and Vibration*, 261(3), pp. 465–481.

[19] Harland, N.R., Mace, B.R. and Jones, R.W.,2001. Adaptive-Passive Control of Vi-

bration Transmission in Beams Using Electro/ Magnetorheological Fluid Filled Inserts, *IEEE Transactions on Control Systems Technology*. 9(2) pp. 209–220.

[20] Yeh, J.Y., Chen, J.Y. Lin, C.T. and Liu, C.Y., 2009. Damping and Vibration Analysis of Polar Orthotropic Annular Plates with ER Treatment, *Journal of Sound and Vibration*, 325(1), pp. 1-13.

[21] Ramkumar, K. and Ganesan, N., 2009. Vibration and Damping of Composite Sandwich Box Column with Viscoelastic/Electrorheological Fluid Core and Performance Comparison, *Materials and Design*, 30(8), pp. 2981–2994.

[22] Rajamohan, V., Sedaghati, R. and Rakheja, S.,2010. Vibration Analysis of a Multi-Layer Beam Containing Magnetorheological Fluid, *Smart Mater. Struct*, 19(1), pp. 1-12.

[23] Ghasemi, A.R. and Meskini, M.,2019. Free vibration analysis of porous laminated rotating circular cylindrical shells. *Journal Vibration Control*. ,25(18), pp. 2494–2508.

[24] Rajamohan, V., Rakheja, S. and Sedaghati, R.,2010. Vibration Analysis of a Partially Treated Multi-Layer Beam with Magnetorheological Fluid, *Journal of Sound and Vibration*, 329(17), pp. 3451–3469.

[25] Rajamohan, V. Sedaghati, R. and Rakheja, S., 2010. Optimum Design of a Multilayer Beam Partially Treated with Magnetorheological Fluid, *Smart Mater. Struct*, 19(6), pp. 58-73.

[26] Frostig, Y., Thomsen, O.T, 2004. Higher-order free vibration of sandwich panels with a flexible core. *International Journal of Solids and Structures*, 41(5), pp.1697–1724.

[27] Malekzadeh, k., Livani,M., Ashenai Ghasemi,F. 2014. Improved high order free vibration analysis of thick double-curved sandwich panels with transversely flexible cores. *Latin American journal of solids and structures*, 11(12), pp. 2284–2307.

[28] Yalcintas, M. and Coulter, J. P., 1995. Analytical modeling of electrorheological material based adaptive beams. *Journal of Intelligent Material Systems and Structures*, 6(4), pp. 488-497.

[29] Reddy, J.N., 1987. A Refined Nonlinear Theory of Plates with Transverse Shear Deformation, *Int J Solids Struct*, 20(9), pp. 881–896.

[30] Vinson, J.R. ,1986. Optimum Design of Composite Honeycomb Sandwich Panels Subject to Uniaxial Compression, *AIAA Journal*, 24(10), pp. 1690-1696.

[31] Sanders, J.R., Lyell, j., 1959.An Improved First Approximation Theory for Thin Shells, NASA THR24.

[32] Reddy, J.N., 2004. Mechanics of Laminated Composite Plates and Shells, Theory and Analysis, Second Edition, New York, CRC Press.

[33] Asgari, M., 2010. Optimization Design of Sandwich Panel with MR Layer Using High-Order Theory, M. Sc. Thesis, Aerospace College, K.N. University. (in Persian).

[34] Hasheminejad, S.M., Maleki, M., 2009. Free vibration and forced harmonic response of an electrorheological fluid-filled sandwich plate, *Smart Materials and Structures*. 18(5), pp. 055013.